Journal of Plant Physiology 220 (2018) 60–68

Contents lists available at ScienceDirect

Journal of Plant Physiology

journal homepage: www.elsevier.com/locate/jplph

Research Paper

Xylella fastidiosa induces differential expression of lignification related-genes and lignin accumulation in tolerant olive trees cv. Leccino

Erika Sabella, Andrea Luvisi*, Alessio Aprile, Carmine Negro, Marzia Vergine, Francesca Nicolì, Antonio Miceli, Luigi De Bellis

Department of Biological and Environmental Sciences and Technologies, University of Salento, via Prov.le Monteroni 165, 73100 Lecce, Italy

ARTICLE INFO

Keywords:
Olive quick decline syndrome
CoDiRO
Lignin
Leccino
Quinic acid
Hydroxytyrosol glucoside

ABSTRACT

Recently, *Xylella fastidiosa* was reported in Italy, associated with the "Olive Quick Decline Syndrome". The cv. Leccino exhibits an evident tolerance with a slow disease progression compared with the other cultivars. Between the mechanisms proposed to explain the putative tolerance of some hosts to *X. fastidiosa* diseases, lignin deposition plays an important role. Analysis of phenolic compounds in healthy and infected Leccino and Cellina di Nardò leaves showed, in the two cultivars, a reduction of hydroxytyrosol glucoside (usually associated with drought and cold stress) and, only in Leccino, an increase of quinic acid, precursor of lignin. To determine if lignin biosynthesis is involved in defence response, we investigated the expression of genes coding for entry-point enzymes in different branches of the phenylpropanoid pathway. In stems of Cellina di Nardò infected plants, *Cinnamate-4-Hydroxylase* (*C4H*) and *4-Coumarate:CoA Ligase* (*4CL*) resulted strongly down-regulated, indicating a plant disease response since the inhibition of *C4H* is reported to promote the accumulation of benzoic acid and salicylic acid as defence signals. Instead, in the cv. Leccino, *Cinnamoyl-CoA Reductase* (*CCR*, reported to be strongly induced during the formation of lignin defence response associated) was up-regulated in the stem of infected plants; moreover, *Polyphenol oxidase* (*PPO*), coding for an enzyme involved in the hydroxytyrosol biosynthesis, was down-regulated. The quantification of lignin in healthy and infected branches of both cultivars, showed a significant increase of total lignin in infected Leccino compared with the sensitive cultivar; moreover, histochemical observations of stem sections exhibited a different lignin distribution in the sclerenchyma and in the xylem tissue of infected Leccino plants compared to sections of healthy ones. Results suggest a critical role for lignin in *X. fastidiosa* tolerance of cv. Leccino.

1. Introduction

Xylella fastidiosa is a pathogenic bacterium causing diseases in many crop species and it leads to considerable economic loss (Tumber et al., 2014; Luvisi et al., 2017a). The management of these diseases is difficult because the vascular colonization of plants by the pathogen limits its accessibility to bactericides. Therefore, recent research focused on the understanding the host inhibition of bacterial growth which leads to host tolerance. Particular attention has been given to xylem-localized phenolic compounds that are associated to anti-*Xylella* activity as evaluated using in vitro assays (Wallis and Chen, 2012; Maddox et al., 2010). Nevertheless, the role of phenolic compounds in the natural defense or resistance mechanisms of plants is usually evaluated in relation to their antimicrobial activities underestimating their role as precursors of other compounds; for this purpose, lignin deserves special mentioning. An increase in the synthesis of lignin was found in response to many pathogens and the central role of lignin metabolism in plant resistance is demonstrated (Xu et al., 2011; Gayoso et al., 2010; Miedes et al., 2014; Wallis and Chen, 2012). Also for *X. fastidiosa*, the role of xylem anatomy in affecting bacteria intra-plant movement has been confirmed (Chatelet et al., 2011; Sun et al., 2011). Baccari and Lindow (2010) examined grape cultivars that differ in their susceptibility to this disease and they found that *X. fastidiosa* reached much lower population sizes and colonized fewer xylem vessels in the stem of resistant cultivars compared with more susceptible cultivars. In contrast, vessels of petioles are colonized from bacteria in a similar proportion suggesting that resistance to Pierce's disease is apparently not due to inhibitory compounds that circulate in the xylem but the movement of *X. fastidiosa* from an infected vessel to an adjacent one employs the degradation of the pit membrane and grape cultivars that are most easily digested by *X. fastidiosa* enzymes will be more easily invaded (Baccari and Lindow, 2010). The pit membrane was composed of crystalline

* Corresponding author.
E-mail address: andrea.luvisi@unisalento.it (A. Luvisi).

https://doi.org/10.1016/j.jplph.2017.10.007
Received 6 July 2017; Received in revised form 25 October 2017; Accepted 27 October 2017
Available online 10 November 2017
0176-1617/

cellulose and lignins (Herbette et al., 2015), thus increased levels of these compounds in xylem vessels could suggest that cell walls of infected plants become more specialized in order to limit the ability of the *X. fastidiosa* to move into the adjacent vessel delaying disease progression.

From the October 2013, *X. fastidiosa* was reported under field conditions in Italy (Apulia region), associated with severe cases of the "Olive Quick Decline Syndrome" (OQDS) (Saponari et al., 2013).

The most widespread South Apulia traditional cultivars Cellina di Nardò and Ogliarola di Lecce appear to be sensitive enough to die when infected (Frisullo et al., 2014; Martelli, 2016), while in the course of field surveys, it was repeatedly observed that cv. Leccino had a healthy look and a green canopy with very little leaf scorching (Martelli, 2016; Luvisi et al., 2017b).

To better understand the processes contributing to the putative *X. fastidiosa* tolerance of olive trees cv. Leccino, this current study examines, in the two cultivars Leccino and Cellina di Nardò, changes in phenolic compound production and expression of genes coding for enzymes involved in lignin biosynthetic pathway; finally, lignin quantification and histochemical analysis of lignin in xylem vessels aims to evaluate whether lignification of cell walls can be a key event to explain tolerance in the cv. Leccino.

2. Materials and methods

2.1. Experimental design

Trials were carried out in orchards located in Province of Lecce (Parco Naturale Regionale Bosco e Paludi di Rauccio, 40°27′24.0"N 18°09′43.8"E, Apulia, Italy), in which olive trees of cv. Leccino and Cellina di Nardò were monitored since 2015. Selected plants (25–35 years) were characterized from the same agronomic practices in the last 5 years. Management practices in 2016 were the same for all plants. After winter pruning of trees, the canopy was not pruned during vegetative growth. Phytosanitary treatments were carried out according to EU Decision 2015/789. The decision declare that in the Province of Lecce the pathogen is already widely established and calls for containment measures that should aim to reduce the amount of bacterial inoculum in that area and keep the vector population (*Philaenus spumarius*) at the lowest level possible. Control of common insects such as *Bactrocera oleae* was also carried out in order to minimize the effects of other pests. Orchards were also weekly monitored to detect eventual insect or other pest outbreaks. According to Alagna et al. (2012), to avoid possible effects of different levels of water availability on the phenolic content among trees, tree water status was assessed by Ψ_w measured every two weeks using a pressur chamber (Gucci et al., 1999). No irrigation were needed.

Leaf samples were collected from 12 plants per cultivar belonging to infected areas and from 12 plants per cultivar belonging to non-infected areas. In April, July and October 2016, leaf samples (25 leaves collected from six branches per plant) were collected to asses *X. fastidiosa* presence by PCR (Rodrigues et al., 2003). Further leaf samples collected in April, July and October 2016 from the same plants were also used for phenolic analyses. In April 2016, stem tissues from the same plants of *X. fastidiosa* assay were also collected to analyse the expression of genes involved in different branches of the phenylpropanoid and the lignin biosynthesis pathways. Stem sections of the same samples were also used for quantification of lignin content and for histochemical analysis.

Samples from infected groups were always collected only from branches showing characteristic leaf scorching symptoms (scorched leaf tip) to limit effects due to mixed infections of other pathogens with *X. fastidiosa*, whereas samples from not-infected groups were collected if symptoms due to other biotic or abiotic stress were note showed.

Leaf samples used for the phenolic composition assay, expression gene analysis, quantification of lignin content and for histochemical analysis were collected from branches which leaves were also assayed by qPCR for widespread leaf olive pathogens such as *Verticillium dahliae* (Bilodeau et al., 2012), *Colletotrichum* spp., *C. acutatum* and *C. gloeosporioides* (Garrido et al., 2009), to ensure that differences found in phenolic composition were not influenced by mixed infections with other pathogens. The most common woody fungal species associated with olive wilt and decline in Southern Italy, *Phaeomoniella chlamydospora*, *Phaeoacremonium aleophilum* and *P. parasiticum* (Carlucci et al., 2015) were also assayed by qPCR, using wood chips obtained from branches (Aroca et al., 2008; Martín et al., 2012). Wood chips were also tested by PCR for *Botryosphaeria dothidea* (Romanazzi et al., 2009), *Diplodia seriata* (Martín et al., 2014). *Phytophthora* spp., previously detected in South Italy (Cacciola et al., 2001), was also checked in woody chips (Drenth et al., 2006). Trees positive to tests against previously described pathogens were not used for phenolic composition assay, expression gene analysis, quantification of lignin content and for histochemical analysis.

2.2. DNA extraction and PCR

To evaluate the presence of *X. fastidiosa* in olive trees, 25 leaves were collected from six branches per plant and, for each sample, leaf petioles and basal portions of leaf blades were cut with a sterile scalpel. Plant tissue from each sample (approx. 1 g of leaf petioles) was transferred into an extraction bag (BIOREBA, Switzerland) and 4 mL of extraction buffer (0.2 M Tris–HCl pH 9, 0.4 M LiCl and 25 mM EDTA) were added. Sample homogenization was performed using a semi-automatic homogenizer (Homex 6, BIOREBA) at 50% maximum speed. DNA extraction was performed following the protocol of Edwards et al. (1991) which described the most commonly used method of purifying and concentrating DNA from samples. In this protocol, the DNA solution is first extracted with a phenol/chloroform/isoamyl alcohol mixture to remove protein contaminants and then precipitated with 100% ethanol.

The isolated DNA was used as template for *X. fastidiosa* detection by PCR with the primers X.fas-0838-a-S-21-X.fas-1439-a-A-19 and XYgyr499-RXYgyr907 (Rodrigues et al., 2003). Amplification was performed in a 25 µL reaction containing 0.2 µM concentrations of each primer, 200 µM concentrations of dNTPs, 1 x Taq buffer, 2.0 U of *Taq* DNA polymerase (TaKaRa, Kyoto, Japan), and 100 ng of DNA template. The PCR was initiated with a 3 min denaturation step at 94 °C, followed by 30 cycles of denaturation at 94 °C for 1 min, primer annealing at 55 °C for 30 s, extension at 72 °C for 2 min, and final extension for 7 min. Positive and negative samples were also assayed by TaqMan real-time PCR protocol with XF-F/R primers and XF-P probe (Harper et al., 2010). Reactions were performed in a real-time thermal cycler (ABI PRISM 7900HT, Applied Biosystems). Each reaction consisted of 5 µL from a 20 ng µL-1 dilution of DNA extracted from 1 g of leaf petioles, 12.5 µL of Master Mix (Applied Biosystems), 400 nM forward and reverse primers, 200 nM TaqMan probe, ultrapure DNase/RNase-free water (Carlo Erba Reagents S.r.l.) in a total volume of 25 µL. The cycling conditions were: an initial denaturation step at 95 °C for 10 min, followed by 40 cycles of 95 °C for 15 s and 60 °C for 1 min, with the final dissociation at 95 °C for 15 s, 60 °C for 30 s and 95 °C for 15 s.

2.3. Phenolic analyses

Immediately after harvesting, leaves were frozen in liquid nitrogen and stored at −80 °C until further analysis. Extraction and analysis of phenolic compounds were carried out following Taamalli et al. (2012). Ten milliliters of a mixture of methanol and water (80:20, v/v) was added to 1 g of fresh milled olive leaves, and the sample was maintained 24 h in the dark at room temperature. The extracts were centrifuged at 5000*g* for 10 min and then filtered through a 0.45 µm syringe filter prior to analysis. Total phenolic compounds were assayed via spectrophotometric method Fast Blue BB (4-benzoylamino-2,5-dimethoxybenzenediazonium chloride hemi-[zinc chloride]) salt), using

Table 1
Primers used for RT-PCR to measure expression levels of phenylpropanoid pathway genes.

Gene name	Name	sequence 5′-3′	Reference	GenBank
B-Actin	***β-Act_F***	ACTATGAACAGGATCTTGAG	Rossi et al. (2016)	AF545569.1
	β-Act_R	GAACCACCACTGAGGACGAT	Rossi et al. (2016)	AF545569.1
Cinnamate-4-Hydroxylase	***C4H_F***	CGGCATTACTTTGGGACGTTT	Corrado et al. (2012)	JQ711532.1
	C4H_R	GCAGACTGAATTGGCCACCT	Corrado et al. (2012)	JQ711532.1
Phenylalanine-Ammonia-Lyase	***PAL_F***	CCTCCGTGGAACAATCAGTT	Alagna et al. (2012)	JX266201.1
	PAL_R	CTCAGCCGTCAAGGATTCTC	Alagna et al. (2012)	JX266201.1
4-Coumarate:CoA Ligase	***4CL_F***	AACAAGTTGATGGGGAAAAT	Alagna et al. (2012)	JX266203.1
	4CL_R	ATCCACACAGCAGCACAGAA	Alagna et al. (2012)	JX266203.1
Chalcone Synthase	***CHS_F***	ACCGGATGACACTCATTTGGA	Ferrante et al. (2004)	AF384049.1
	CHS_R	GCGCCGTCGCCAAAC	Ferrante et al. (2004)	AF384049.1
Chalcone Isomerase	***CHI_F***	CGTTTAACGGGTCCACAGTACTCA	Rossi et al. (2016)	GU646679.1
	CHI_R	GCTTTCCAATGCGCAACAC	Rossi et al. (2016)	GU646679.1
Cinnamoyl-CoA Reductase	***CCR_F***	TCAGAGGCACCGTCAGAAATC	Koudounas et al. (2015)	ACD13265.1
	CCR_R	GTAAACTCTCTCGAACTTCCTCG	Koudounas et al. (2015)	ACD13265.1
Polyphenol oxidase	***PPO_F***	*ACATTGCCTCCCATTTTCGATA*		JX266193.1
	PPO_R	*ACTACGTTTAGCCCTAGGT*		JX266193.1
Peroxidase	***POD_F***	*AAAGGACGAAAAGATGGACGAATA*		GQ851609.1
	POD_R	*GTTAACGGTAAAGGTTGGAAG*		GQ851609.1

gallic acid standard dilution (Medina, 2011). Phenolic characterization (Taamalli et al., 2012; Taamalli et al., 2013; Fu et al., 2010; Talhaoui et al., 2014; Quirantes-Piné et al., 2012) was carried out using an Agilent 1200 Liquid Chromatography system (Agilent Technologies, Palo Alto, CA, USA) equipped with a standard autosampler. The HPLC column was an Agilent Extended C18 (1,8 µm, 2,1 × 50 mm). Separation was carried out at 40 °C with a gradient elution program at a flow rate of 0.5 mL/min. The mobile phases consisted of water plus 0.1% formic acid (A) and acetonitrile (B). The following multistep linear gradient was applied: 0 min, 1% B; 13 min, 25% B; 19 min, 40% B; 21 min, 90% B. The initial conditions were maintained for 5 min. The injection volume in the HPLC system was 5 µL. The HPLC system was coupled to an Agilent 6320 TOF mass spectrometer (Agilent Technologies, Palo Alto, CA, USA) equipped with a dual ESI interface (Agilent Technologies, Palo Alto, CA, USA) operating in negative ion mode using a capillary voltage of +3.5 kV. The other optimum values of the ESI–TOF–MS parameters were drying gas temperature, 300C; drying gas flow, 12 L/min; and nebulising gas pressure, 40 psig. Detection was carried out within a mass range of 50–1700 *m/z*. The accurate mass data of the molecular ions were processed through the software Mass Hunter (Agilent Technologies, Palo Alto, CA, USA).

2.4. Quantification of phenolic compounds

Five standard calibration graphs for the quantification of the phenolic compounds of olive leaves were prepared using commercial standards (quinic acid, oleuropein, hydroxytyrosol, luteolin and luteolin 7-*O*-glucoside) (Sigma-Aldrich, Saint Louis, MO, USA). Standards were dissolved a mixture of methanol and water (80:20, v/v) and diluted in water plus 0.1% formic acid and 1% acetonitrile.

The hydroxytyrosol-glucoside content was estimated using the analytical curve for hydroxytytosol, while the analytical curve of oleuropein was used to estimate contents of all secoiridoids (secologanoside, oleuropein aglycone, oleuropein diglucoside, 2-methoxy oleuropein). Analytical recoveries for compounds for which pure standards were available were assessed by adding to the milled fresh leaves/methanol solution an amount of standard that was 5-times higher than endogenous concentration. The experiment was done in triplicate. Data were presented as analytical recovery (%).

To assess the variability of the extraction method the procedure was repeated four times on the same pool of leaves. No statistically relevant difference was found among replicates.

The limit of quantification (LOQ) was determined as the signal-to-noise ratio of 10:1, and the limit of detection (LOD) was determined as signal-to-noise ratio of 3:1. Intraday and interday precision was performed to assess the repeatability of the method, expressed by the relative standard deviation (RSD). An olive-leaf extract was injected (n = 5) on the same day (intraday precision) for 3 consecutive days (interday precision, n = 15).

2.5. Total RNA isolation, cDNA synthesis and RT-PCR analysis of gene expression

Stem tissues (1 cm length of one-year old stem, collected from six branches per plant) of 24 plants for each cultivars (12 negative samples and 12 positive samples to *X. fastidiosa* by end-point PCR, Rodrigues et al., 2003) were collected from the same branches previously analysed and immediately placed in liquid nitrogen. Total RNA was isolated from 0.1 gr of frozen samples using TRIZOL (Invitrogen). cDNA synthesis was performed using TaqMan® Reverse Transcription Reagents (Applied Biosystems, Foster City, USA). Real-time PCR was performed with the Power SYBR Green RT-PCR Master mix (Applied Biosystems) according to the manufacturer's instructions. To calculate the Fold Changes (FC) the following formula was used: FC = 2^-ΔΔCT where

$$\Delta\Delta CT = (CT_{targetgene} - CT_{referencegene})_{\ treatedsample} - (CT_{targetgene} - CT_{referencegene})_{\ controlsample}$$

The CT data are expressed as average of the 12 samples.

The used primers were retrieved from the literature or designed with the software Primer Express Software 3.0 on the mRNA sequences deposited in GenBank (Table 1). The analysed genes code for enzymes involved in the biosynthesis of monolignols and they are shown below. Phenylalanine-Ammonia-Lyase (PAL) is the first enzyme that converts phenylalanine into cinnamic acid and it is transcriptionally regulated in response to many environmental stresses but its activation is organ and genotype dependent (Rossi et al., 2016). The enzyme Cinnamate-4-Hydroxylase (C4H) converts cinnamic acid into *p*-coumaric acid, the immediate precursor of coumarins. 4-Coumarate:CoA Ligase (4CL) is the enzyme that activates 4-coumarate through the binding of ATP and CoA (Rossi et al., 2016). Cinnamoyl-CoA Reductase (CCR) catalyses the first committed step of the lignin-specific branch to produce lignin monomers (Koudounas et al., 2015). Chalcone Synthase (CHS) and Chalcone Isomerase (CHI) are key enzymes which serve at the initial step in flavonoid biosynthesis. Polyphenol oxidase (PPO) catalyses the oxygen-dependent oxidation of phenols to quinones and the products of these reactions are highly reactive molecules that can covalently modify and crosslink a variety of cell molecules to produce, by condensation and accumulation, black or brown polymers. The Peroxidases (POD) are enzymes that catalyze the oxidation of different substrates using H_2O_2; they are active in such physiological processes as ferulate

dimerization, phenol oxidation and lignification (Quiroga et al., 2000).

β-Actin that has been previously shown to have a stable expression in Leccino stem (Rossi et al., 2016) was tested and used for the normalization (Nicot et al., 2005; Maroufi et al., 2010)

2.6. Determination of total lignin content

Total lignin content was determined by the Klason method (Moreira-Vilar et al., 2014). Protein-free cell wall samples were prepared from dry stems from 12 healthy and 12 infected plants for each cultivars; this step is essential to remove protein and other constituents that are measured together with lignin at 280 nm (Moreira-Vilar et al., 2014). Dry samples (0.3 g) were homogenized in 50 mM potassium phosphate buffer (7 mL, pH 7.0) using a mortar and pestle and then transferred into a centrifuge tube. The pellet was centrifuged (1.400 x g, 5 min) and washed by successive stirring and centrifugation as follows: two times with phosphate buffer (pH 7.0; 7 mL), three times with 1% (v/v) Triton X-100 in pH 7.0 buffer (7 mL), two times with 1 M NaCl in pH 7.0 buffer (7 mL), two times with distilled water (7 mL), and two times with acetone (5 mL). The pellet was dried in an oven (60 °C, 24 h) and cooled in a vacuum desiccator. The dry matter obtained was defined as the protein-free cell wall fraction. To determine the lignin content, 1.0 g of the protein-free fraction was digested (72% H2SO4, 47 °C, 7 min) under vigorous stirring. After complete digestion, the sample was autoclaved (121 °C, 1 atm, 30 min), followed by filtration through filter paper to separate the soluble and insoluble fractions. The soluble fraction was measured at 280 nm and 215 nm, and the soluble lignin content was calculated by the following formula: S = (4.53 A215–A280)/300. Ash content of all samples was determined by combustion of the insoluble fraction for 4 h. Lignin from the insoluble fraction was calculated by the difference in the weight of the dry mass and the total ash for each sample. The lignin content was determined by the sum of the insoluble and soluble lignin and it was expressed as mg g^{-1} cell wall.

2.7. Tissue staining

Thin sections of the stem (one-year-old) were stained with Calcofluor white M2R (which is used to detect cellulose) and Safranin O (which detects lignin deposition). The following stain solutions were prepared: Calcofluor White M2R (Sigma-Aldrich) 0.02% (w/v) in distilled water and Safranin O (Sigma-Aldrich,) 0.5% (w/v) dissolved in 50% EtOH. Staining with Calcofluor White M2R was performed according to Mitra and Loqué (2014). Stained sections were excited at 395 nm and imaged using a filter of 420 nm. Staining with Safranin O was performed according to Bond et al. (2008). Stained sections were excited at 492 nm and imaged using a filter of 520 nm.

All images were taken on a confocal laser-scanning microscope (Carl Zeiss LSM 700 laser scanning microscope, Jena, Germany); all images were acquired with the same microscope settings and analyzed with the Zeiss LSM image examiner software 4.2.0.121.

2.8. Statistical analyses

The open source software R ver.3.3.1 (R Foundation for Statistical Analysis) and the package “agricolae” version 1.2–8 (De Mendiburu, 2017) was used for all data analyses. For normally distributed data, one-way or two-way analysis of variance (ANOVA) and pairwise multiple comparisons, using Duncan’s test, were applied (P-value ≤ 0.05 was considered to be significant). The Student *t*-test was used to test the statistical significance of the differences found in the expression profile of genes coding for enzymes involved in the phenylpropanoid pathway and for the lignin content. Principal component analysis (PCA) was done on data relative to phenolic compounds and gene expression to determine to what extent the variables considered in the experiment can explain the variation in our dataset.

3. Results and discussion

3.1. Phenolic analyses

The calibration plots indicated good correlations between peak areas and analyte concentrations, and the regression coefficients were higher than 0.988 in all cases. LOD was found to be within the range 0.002 and 0.005 mg/mL while LOQ was within 0.005 and 0.009 mg/mL. The highest intraday repeatability of the peak area among all peaks, expressed by RSD, was 0.82%, whereas the highest interday repeatability among all peaks was 1.1%. The different parameters of the calibration curves are summarized in Supplementary Table S1. Characterization of olive leaf extract by HPLC-ESI-TOF was reported in Table 2 (April dataset). Compounds showed in Table 2 were found in leaves sampled during each period.

Differences in constitutive levels of phenols among sampling period were observed in Leccino (Table 3) and in Cellina di Nardò (Table 4). In particular, oleuropein diglucoside, 2-methoxy oleuropein, luteolin (only in the cv. Leccino) and oleuropein showed similar trends, characterized by higher compound contents in spring and autumn compared to summer. Quinic acid showed a specular behavior, due to higher values observed during summer. The content of hydroxytyrosol glucoside decreased with seasons’ progression.

fastidiosa-positive samples showed significant differences in quinic acid and hydroxytyrosol glucoside levels in the cv. Leccino (Table 3), while in the cv. Cellina di Nardò differences were observed only in hydroxytyrosol glucoside (Table 4). In the cv. Leccino, quinic acid was significantly higher in infected leaves compared to healthy one in spring (+115%) and autumn (+81%), while no difference was observed in leaves sampled in summer. In the two cultivars, the content of hydroxytyrosol glucoside was almost depleted in infected leaves regardless period of sampling; our data follow the same trend found for hydroxytyrosol glucoside in response to other environmental stress. Petridis et al. (2012) demonstrated that in all olive cultivars hydroxytyrosol levels significantly decreased with water stress and the same observation was reported by Ortega-Garcìa and Peragòn (2009) in the cultivar Picual in response to cold stress.

Other quantified compounds did not differ according to health status or sampling period.

Data obtained from the cv. Leccino were in accordance with observations reported in Pierce’s disease, since quinic acid occurs at great levels in xylem tissues of the grapevine infected by *Xylella fastidiosa* and it is the only phenolic compound significantly associated with the Pierce’s disease (Wallis and Chen, 2012; Wallis et al., 2013). Quinic acid is a precursor in lignin biosynthesis (Barros et al., 2015). Lignification has been proposed as a general mechanism of resistance on the basis of a number of experiments in which lignification was found in resistant varieties of the host plants but not in the susceptible ones after the pathogen inoculation, showing that resistant plants accumulated lignin more rapidly and/or exhibited enhanced lignin deposition as compared with susceptible plants (Miedes et al., 2014; Xu et al., 2011; Gayoso et al., 2010). These results may indicate a likely participation of lignin in Leccino response to *X. fastidiosa*.

3.2. Expression of lignification related-genes in X. fastidiosa infected olive plants

Lignin monomer precursors derive from the aromatic amino acid phenylalanine, synthesized in the plastid, which is converted into 4-hydroxyphenylpropene alcohols (Barros et al., 2015). The lignin biosynthetic pathway is relatively well described in many species; in order to evaluate if there is a perturbation of lignin biosynthetic pathway in *X. fastidiosa* infected Leccino plants in comparison to healthy plants and to the sensitive cv. Cellina di Nardò, the expression of genes coding for enzymes involved in the biosynthesis of monolignols was analyzed (Fig. 1A and B). The results of this experiment showed that in the cv.

Table 2
Characterization of olive leaf extract by HPLC-ESI-TOF (ion M-H)$^-$. Exp = experimental; Clc = calculated.

Peak	Compound	RT (min)	(M−H)$^-$ Exp	*m/z* Exp	*m/z* Clc	[a]Diff. (ppm)	[b]Score	[c]Reference
1	[d]Quinic acid	0.365	$C_7H_{11}O_6$	191.0571	191.0561	−5.89	90.44	1, 2, 3
2	[d]Hydroxytyrosol glucoside	2.965	$C_{14}H_{19}O_8$	315.1095	315.1085	−1.26	96.62	1, 2, 3
3	Secologanoside is 1	3.960	$C_{16}H_{21}O_{11}$	389.1095	389.1089	−1.11	88.91	1, 2, 3
4	Secologanoside is 2	6.116	$C_{16}H_{21}O_{11}$	389.1101	389.1089	−2.62	96.13	2
5	Elenoic acid glucoside	6.630	$C_{17}H_{23}O_{11}$	403.1262	403.1246	−3.68	80.9	2
6	Oleuropein aglycon derivate	7.194	$C_{16}H_{25}O_{10}$	377.1459	377.1453	−1.23	92.94	2
7	Unknown	7.825	$C_{19}H_{27}O_{10}$	415.1621	415.1610	−2.44	95.92	2
8	Hydroxyolouropein	9.036	$C_{25}H_{31}O_{14}$	555.1732	556.1803	−2.04	97.55	2, 4
9	[d]Luteolin 7-*O*-glucoside is. 1	9.119	$C_{21}H_{19}O_{11}$	447.0952	447.0933	−3.93	77.64	3, 2
10	Luteolin rutinoside	9.517	$C_{27}H_{29}O_{15}$	593.1517	593.1512	−0.87	97.79	3
11	[d]Luteolin 7-*O*-glucoside is. 2	9.998	$C_{21}H_{19}O_{11}$	447.0948	447.0933	−3.03	96.13	1, 2, 3
12	Apigenin 7 glucoside	10.010	$C_{21}H_{19}O_{10}$	431.0988	431.0984	−0.79	97.82	1, 2, 3
13	Oleuropein diglucoside is. 1	10.545	$C_{31}H_{41}O_8$	701.2307	701.2298	−0.6	93.83	1, 2, 3
14	Oleuropein diglucoside is. 2	10.728	$C_{31}H_{41}O_8$	701.2306	701.2298	−0.49	94.85	1, 2, 3
15	Oleuropein diglucoside is. 3	10.893	$C_{31}H_{41}O_8$	701.2291	701.2298	3.2	98.67	1, 2, 3
16	2-methoxy oleouropein is. 1	11.175	$C_{26}H_{33}O_{14}$	569.1898	569.1876	−3.76	85.77	3
17	2-methoxy oleouropein is. 2	11.258	$C_{26}H_{33}O_{14}$	569.1899	569.1876	−3.64	97.16	3
18	Oleuropein	11.406	$C_{25}H_{32}O_{13}$	539.1772	539.1770	0.03	97.14	1,2,3,4
19	[d]Luteolin	11.939	$C_{15}H_9O_6$	285.0419	285.0405	−4.87	97.08	1,2,3,4
20	Ligstroside	12.611	$C_{25}H_{31}O_{12}$	523.1823	523.1821	−0.03	97.55	5
21	[d]Apigenin	13.382	$C_{15}H_9O_5$	269.0461	269.0455	−1.77	98.7	1
22	Diosmetin	13.929	$C_{16}H_{11}O_6$	299.0566	299.0561	−1.43	98.5	1

[a] Relative difference: the difference between the observed mass and the theoretical mass of the compound (ppm).
[b] Isotopic abundance distribution match: a measure of the probability that the distribution of isotope abundance ratios calculated for the formula matches the measured data.
[c] Reference list: 1 = Taamalli et al. (2013); 2 = ; Fu et al. (2010); 3 = ; Taamalli et al. (2012); 2 = ; Talhaoui et al. (2014); 5 = ; Quirantes-Piné et al. (2012).
[d] Confirmed by authentic chemical standard.

Leccino *PAL*, *C4H* and *4CL* transcripts did not significantly change in response to the *X. fastidiosa* infection (Fig. 1B), whereas in stems of Cellina di Nardò infected plants, *C4H* (fold change = − 6.54 ± 0.01) and *4CL* (fold change = − 3.71 ± 0.04) resulted strongly down-regulated (Fig. 1B), indicating a plant disease response, since the inhibition of *C4H* is reported to promote the accumulation of defence

Table 3
Levels of phenolic compounds (mg g^{-1} FW) in Leccino olive leaves infected by *X. fastidiosa* (I) compared to negative samples (H). Two-way ANOVA was carried out to evaluate statistical differences and interaction among factors (period of sampling, PS; health status, HS). Letters indicate statistical groups that differ significantly (Duncan's test, P ≤ 0.05).

	Spring		Summer		Autumn		Statistical analysis		
Phenolic compound	H	I	H	I	H	I	PS	HS	PS x HS
01. Quinic acid	1.36 (0.58)^b	2.93 (0.43)^a	3.01 (0.79)^a	3.48 (0.64)^a	1.85 (0.76)^b	3.34 (0.25)^a	***	***	***
02. Hydroxytyrosol glucoside	8.95 (2.77)^a	0.05 (0.07)^c	3.21 (2.26)^b	0.23 (0.05)^c	1.13 (0.35)^b	0.33 (0.13)^c	***	***	***
03. Secologanoside	0.08 (0.05)	0.08 (0.04)	0.07 (0.05)	0.06 (0.06)	0.08 (0.07)	0.06 (0.05)	NS	NS	NS
05. Oleuropein aglycone	0.27 (0.10)	0.33 (0.13)	0.28 (0.11)	0.29 (0.14)	0.26 (0.12)	0.28 (0.09)	NS	NS	NS
08. Luteolin 7-*O*-glucoside	0.61 (0.17)	0.58 (0.15)	0.51 (0.12)	0.53 (0.09)	0.46 (0.13)	(0.49) (0.11)	NS	NS	NS
10. Oleuoropein diglucoside	0.12 (0.02)^a	0.11 (0.03)^a	0.03 (0.02)^b	0.02 (0.02)^b	0.08 (0.03)^a	0.09 (0.03)^a	***	NS	NS
12. 2-methoxy oleouropein	0.35 (0.10)^a	0.34 (0.11)^a	0.12 (0.05)^b	0.13 (0.04)^b	0.27 (0.08)^a	0.29 (0.07)^a	***	NS	NS
14. Luteolin	0.06 (0.01)^a	0.06 (0.01)^a	0.01 (0.01)^c	0.01 (0.01)^c	0.03 (0.01)^a	0.03 (0.01)^a	***	NS	NS
18. Oleuropein	0.35 (0.08)^a	0.38 (0.09)^a	0.16 (0.07)^b	0.15 (0.10)^b	0.40 (0.11)^a	0.38 (0.12)^a	***	NS	NS
Total polyphenols	19.51 (3.78)	20.36 (2.99)	22.03 (4.12)	21.12 (3.56)	22.78 (4.33)	21.09 (3.66)	NS	NS	NS

NS = Not significant;
*** = P < 0.001.

Table 4
Levels of phenolic compounds (mg g^{-1} FW) in Cellina di Nardò olive leaves infected by *X. fastidiosa* (I) compared to negative samples (H). Two-way ANOVA was carried out to evaluate statistical differences and interaction among factors (period of sampling, PS; health status, HS). Letters indicate statistical groups that differ significantly (Duncan's test, P ≤ 0.05).

	Spring		Summer		Autumn		Statistical analysis		
Phenolic compound	H	I	H	I	H	I	PS	HS	PS x HS
01. Quinic acid	1.68 (0.19)^{ab}	1.86 (0.39)^a	2.75 (0.68)^c	2.90 (0.53)^c	2.16 (0.25)^{ab}	2.19 (0.42)^b	***	NS	NS
02. Hydroxytyrosol glucoside	2.45 (0.25)^a	0.28 (0.09)^d	1.23 (0.25)^b	0.22 (0.10)^d	0.84 (0.17)^c	0.24 (0.08)^d	***	***	***
03. Secologanoside	0.06 (0.07)	0.06 (0.04)	0.08 (0.04)	0.06 (0.06)	0.08 (0.04)	0.08 (0.06)	NS	NS	NS
05. Oleuropein aglycone	0.33 (0.11)	0.32 (0.09)	0.29 (0.08)	0.31 (0.11)	0.29 (0.10)	0.27 (0.10)	NS	NS	NS
08. Luteolin 7-*O*-glucoside	0.62 (0.17)	0.65 (0.14)	0.52 (0.11)	0.53 (0.13)	0.49 (0.14)	0.51 (0.11)	NS	NS	NS
10. Oleuoropein diglucoside	0.11 (0.04)^{ab}	0.13 (0.04)^a	0.03 (0.003)^c	0.02 (0.006)^c	0.08 (0.04)^b	0.09 (0.02)^a	***	NS	NS
12. 2-methoxy oleouropein	0.27 (0.05)^{ab}	0.31 (0.06)^a	0.09 (0.05)^c	0.09 (0.03)^c	0.23 (0.06)^{ab}	0.23 (0.06)^b	***	NS	NS
14. Luteolin	0.02 (0.01)	0.02 (0.01)	0.01 (0.01)	0.01 (0.01)	0.02 (0.01)	0.03 (0.01)	NS	NS	NS
18. Oleuropein	1.05 (0.29)^a	1.19 (0.36)^a	0.54 (0.22)^b	0.49 (0.20)^b	1.32 (0.50)^a	1.06 (0.30)^a	***	NS	NS
Total polyphenols	20.44 (3.12)	22.37 (3.99)	21.14 (2.69)	22.83 (4.10)	20.51 (3.41)	20.01 (3.11)	NS	NS	NS

NS = Not significant;
*** = P < 0.001.

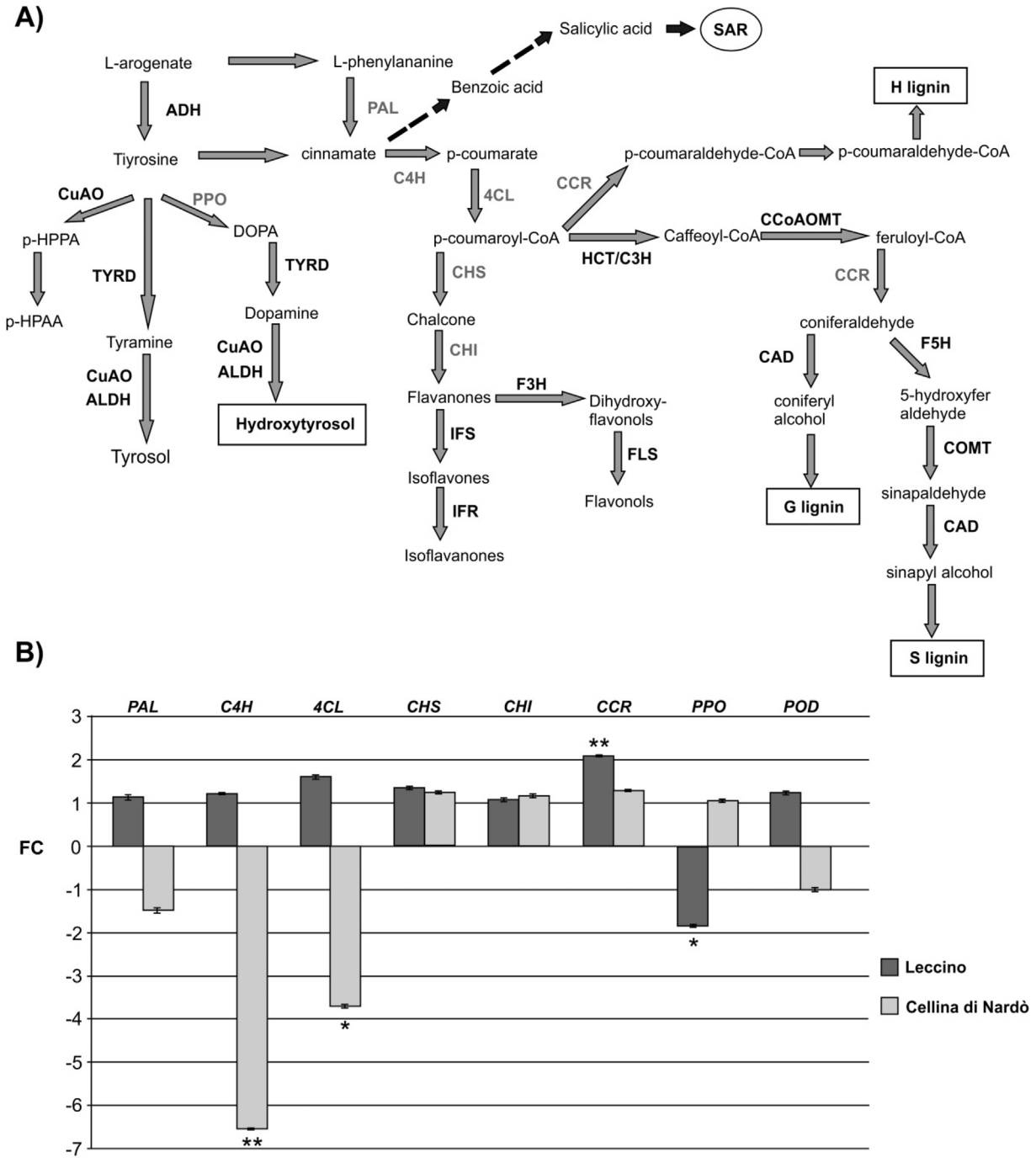

Fig. 1. Expression of lignification related-genes in *X. fastidiosa* infected Leccino and Cellina di Nardò plants. (A) General phenylpropanoid pathway showing in red the analyzed genes. (B) Quantitative analyses of expression of genes coding for entry-point enzymes in different branches of the phenylpropanoid pathway, whereas flux through the pathway may be influenced by levels of enzyme activity. PAL, phenylalanine ammonia-lyase; C4H, cinnamate 4-hydroxylase; 4CL, 4-coumarate:CoA ligase; CCR, cinnamoyl-CoA Reductase; CHS, chalcone synthase; CHI, chalcone isomerase; PPO, polyphenol oxidase; POD, peroxidases. FC: Fold Change. The only significant differences were revealed for the genes coding for the enzyme: CCR and PPO (in the cv. Leccino) and C4H and 4CL (in the cv. Cellina di Nardò) according to Student *t*-test (*p-value $<$ 0,05; ** *p*-value $<$ 0,01).

signals essential for the induction of the Systemic Acquired Resistance (SAR) (Schoch et al., 2002); moreover, *4CL* and *C4H* genes have a common transcriptional activation mechanisms; according to Mizutani et al. (1997) a promoter region of the *C4H* gene reveals elements involved in the regulated expression of *4CL* gene which per se substantiates that *C4H* and *4CL* are coordinately expressed during development and in response to abiotic and biotic stresses such as pathogen infection. An important gene in the lignin formation pathway is *CCR*. The level of expression of *CCR* was higher (fold change = 2.09 ± 0.01) only in stems of infected Leccino plants (Fig. 1B). In *Arabidopsis thaliana At-CCR* has two isozymes coded by different genes: At-*CCR1* that is preferentially expressed during development while At-*CCR2* is expressed at a low level during development but is strongly induced during the defence reaction triggered by the pathogen *Xanthomonas* ssp. and could participate in the formation of stress-induced lignin (Lauvergeat et al., 2001). Similarly, the differential expression of genes coding for enzymes involved in lignin monomer biosynthesis can represent one of the mechanisms contributing to the specific type of

lignin deposited in distinct cell types: during formation of developmental lignin and, more specialized, during formation of pathogen stress-induced lignin.

On the other branch of phenylpropanoid pathway (Fig. 1A), the gene coding for key enzymes in flavonoid biosynthesis *CHS* and *CHI*, in the two analyzed cultivars, remained stable in infected plants in comparison to healthy ones (Fig. 1B).

Polyphenol oxidase (PPO) is another enzyme involved in plant defence against pathogens and stress conditions. *PPO* was down-regulated (fold change = − 1.83 ± 0.03) in infected Leccino plants (Fig. 1B): this result represents a genetic support in relation to the hydroxytyrosol glucoside decrease found with the phenolic compounds analysis in olive leaves infected by *X. fastidiosa*; however, no significant expression differences were found in the cv. Cellina di Nardò suggesting several molecular mechanisms controlling hydroxytyrosol glucoside biosynthesis. In this experiment, an *O. europaea* peroxidase was analyzed but no differences were found in transcripts between infected and healthy Leccino and Cellina di Nardò plants (Fig. 1B); maybe, the reason is that peroxidase activity is the result of the action of a large number of enzymes with similar functions (Gayoso et al., 2010).

In PCAs carried out on phenolic compound and gene expression data set for Cellina di Nardò and Leccino plants, the x-axis explains about the 90% of data set variance (Supplementary Fig. S1,S2). This indicates that almost all variance in the data is explained by PC1 alone. The variation explained by the remaining PCs is very low and might even represent only noise.

3.3. Quantitative analysis of lignin

A significant increase of total lignin was found only in stems of infected Leccino compared with the healthy ones (Fig. 2). In the infected samples of the sensitive cv. Cellina di Nardò no significant lignin increase was detected in comparison with the healthy plants (Fig. 2).

3.4. Lignin and cellulose distribution in X. fastidiosa infected olive plants

Expression analysis of lignin monomer biosynthetic genes and the quantitative analysis of lignin suggest a defence reaction of *X. fastidiosa* infected Leccino plants involving the formation of stress-induced lignin. Differences in lignin distribution were observed by staining cross-sections of the stem with the fluorescent dye Safranin O (Fig. 3A,B,E and F). Due to changes in fluorescence emission, Safranin can differentiate regions of high and low lignin; regions of high lignin fluorescence exhibit an intense yellow/orange color.

Alternatively, the differential lignin distribution can be more easily visualized by the rainbow mode; images were converted to a rainbow scale with the Zeiss LSM image browser to determine the level of saturation, red signals indicate saturation and the point of major lignin deposition, in blue the point of lowest signal intensity. As seen in Fig. 3C and D stem sections of *X. fastidiosa* infected Leccino, exhibit a modified lignin distribution in the sclerenchyma and in the xylem tissue compared to sections of healthy plants: the major anatomical difference is that, in infected plants, the detected signal from stained lignin in the sclerenchyma cells was almost confined to a single row, a well defined ring (Fig. 3B and D); lignin distribution pattern observed in infected Leccino sections was in accordance with the observations of Kraiselburd et al. (2013) in *Citrus sinensis* leaves inoculated with *Xanthomonas citri* subsp. *citri*; they found that in healthy leaves lignin remained mainly distributed around xylem vessels, while in leaves treated with *X. citri* an important lignin accumulation was also observed in the sclerenchymatous fibers. No differences in lignin distribution were observed in infected Cellina di Nardò stem sections (Fig. 3G and H). In the xylem tissue, the cells involved in mechanical support and defence are specialized sclerenchyma cells; these cells are mainly involved in the mechanical support function of xylem and defence against pathogens and herbivores (Aloni et al., 1990). Lignin formation has been suggested as a mechanism of resistance to plant disease and when lignin is required for reinforcing vascular cells, it displaces the aqueous phase of the cell wall, encasing cellulose and matrix polysaccharides and providing enhanced mechanical strength and a water-impermeable barrier (Albersheim et al., 2011). In fact, stem sections of infected and healthy plants were also stained with Calcofluor White which is used to detect cellulose; in sections of infected Leccino plants the staining pattern was dissimilar to that of healthy plants (Fig. 3I and L); in infected plants cellulose deposition appears in a discontinuous pattern compare to sections of healthy plants; so our results suggest that Leccino response to *X. fastidiosa* also affect the deposition pattern of cellulose. In Cellina di Nardò stem sections staining with Calcofluor White, cellulose distribution seemed to remain unchanged in infected and healthy observed samples (Fig. 3M and N).

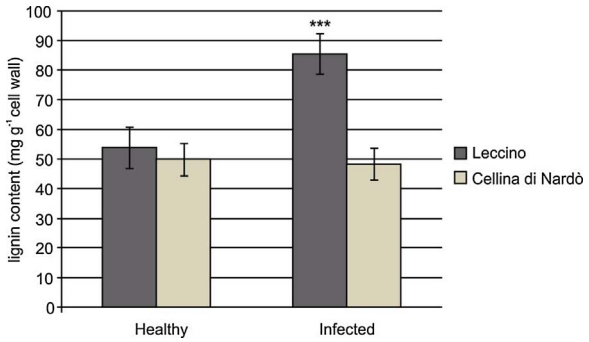

Fig. 2. Total lignin content in stems of healthy and infected Leccino and Cellina di Nardò plants. In the stems of the cv. Cellina di Nardò no differences were found in lignin content; in the cv. Leccino a significant increase of total lignin was detected in infected plants compared with the healthy ones according to Student *t*-test (*p-value < 0,05; ** *p*-value < 0,01; *** *p*-value < 0,001).

4. Conclusion

In a large number of studies, evidence for a role for lignin in plant defense has been obtained also from the analysis of the pathogen resistance of transgenic plants and mutants with contrasting lignin amount. For example, in tomato, the total content of lignin was significantly higher in varieties that were resistant to the vascular bacterium *Ralstonia solanacearum* than in susceptible ones (Miedes et al., 2014). Our report introduces the hypothesis that the putative *X. fastidiosa* tolerance of olive trees cv. Leccino, observed during the field observations, could be influenced by the lignin amount in the xylem vessels that can limit the bacteria movement and the host invasion by slowing down the disease progression. The reported findings provide new insights but a deeper investigation and further studies with artificially inoculated olive trees should produce useful data to confirm our theory.

Author contributions

Conceived and designed the experiments: AL ES LDB AM. Performed the experiments on phenols: CN MV FN. Performed the experiments on pathogens: AL AA ES. Performed the experiments on lignin: ES. Analysed the data: AA ES. Contributed reagents/materials/analysis tools: MV FN. Wrote the paper: AL ES LDB.

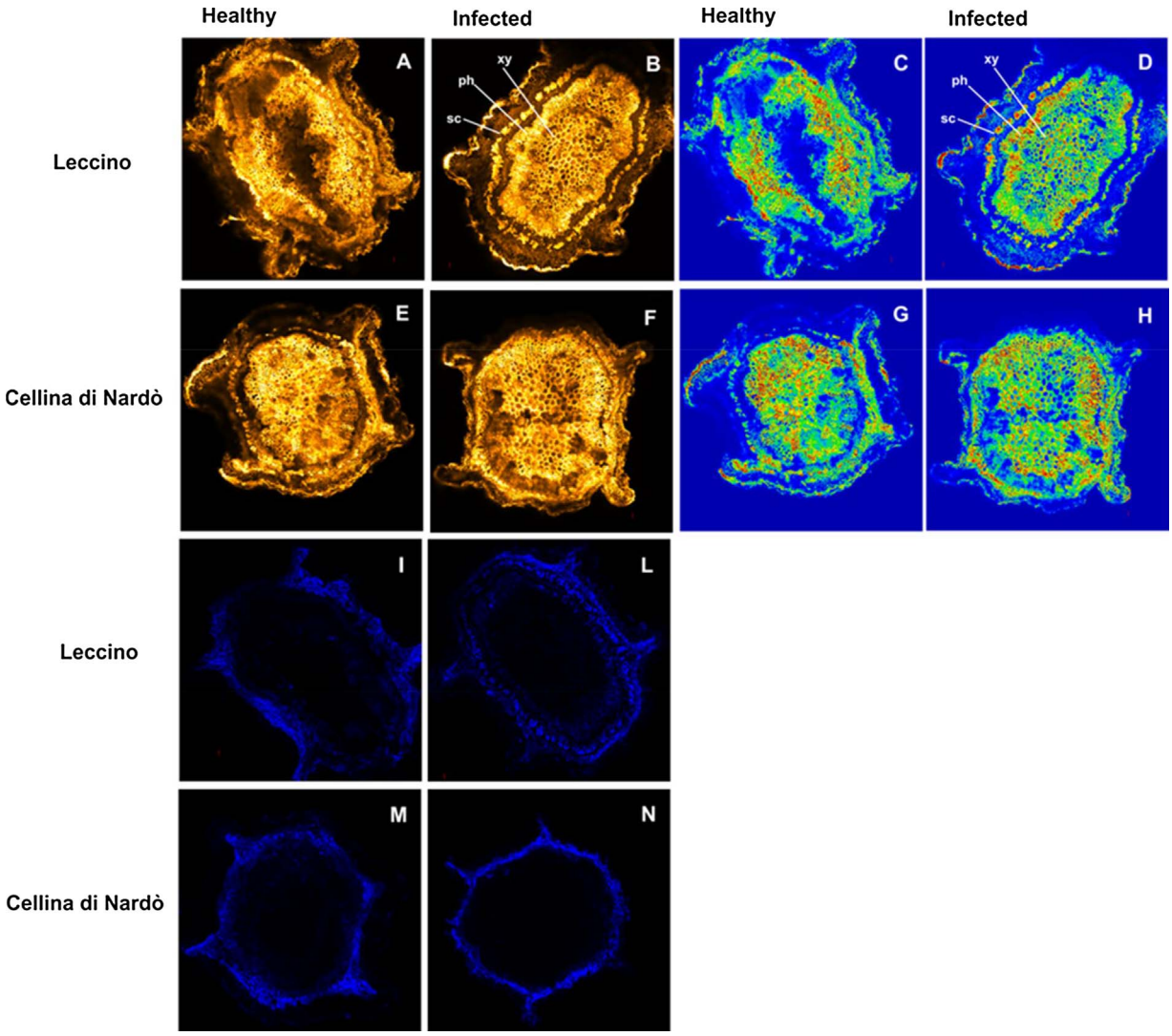

Fig. 3. Lignin and cellulose distribution in stem sections of healthy and *X. fastidiosa* infected olive plants cv. Leccino and Cellina di Nardò. (A, B, E, F) Safranin O-stained stem sections of healthy and infected plants, cv. Leccino and Cellina di Nardò. (C, D, G, H) Intensities of Safranin −O is represented in false rainbow color (highest intensity in red and the lowest intensity in blue). (I, L, M, N) Calcofluor White M2R stained stem sections of healthy and infected plants, cv. Leccino and Cellina di Nardò. sc: sclerenchyma; ph: phloem; xy: xylem. (For interpretation of the references to colour in this figure legend, the reader is referred to the web version of this article.)

Acknowledgments

The work was partially financed by Apulia Region "Cluster Tecnologici Regionali" TAPASS Project. We would like to thank farmers for their support in field observations.

Appendix A. Supplementary data

Supplementary data associated with this article can be found, in the online version, at http://dx.doi.org/10.1016/j.jplph.2017.10.007.

References

Alagna, F., Mariotti, R., Panara, F., Caporali, S., Urbani, S., Veneziani, G., Esposto, S., Taticchi, A., Rosati, A., Rao, R., Perrotta, G., Servili, M., Baldoni, L., 2012. Olive phenolic compounds: metabolic and transcriptional profiling during fruit development. BMC Plant Biol. 12, 162.

Albersheim, P., Darvill, A., Roberts, K., Sederoff, R., Staehelin, A., 2011. Plant Cell Walls, Garland Science. Taylor and Francis Publishing Group, NewYork.

Aloni, R., Tollier, M.T., Monties, B., 1990. The role of auxin and gibberellin in controlling lignin formation in primary phloem fibers and in xylem of *Coleus blumei* stems. Plant Physiol. 94, 1743–1747.

Aroca, A., Raposo, R., Lunello, P., 2008. A biomarker for the identification of four *Phaeoacremonium* species using the *β-tubulin* gene as the target sequence. Appl. Microbiol. Biotechnol. 80, 1131–1140.

Baccari, C., Lindow, S.E., 2010. Assessment of the process of movement of *Xylella fastidiosa* within susceptible and resistant grape cultivars. Phytopathology 101, 77–84.

Barros, J., Serk, H., Granlundz, I., Pesquet, E., 2015. The cell biology of lignification in higher plants. Ann. Bot. 115, 1053–1074.

Bilodeau, G.J., Koike, S.T., Uribe, P., Martin, F.N., 2012. Development of an assay for rapid detection and quantification of *Verticillium dahliae* in soil. Phytopathology 102, 331–343.

Bond, J., Donaldson, L., Hill, S., Hitchcock, K., 2008. Safranine fluorescent staining of wood cell walls. Biotech. Histochem. 83, 161–171.

Cacciola, S.O., Agosteo, G.E., Magnano di San Lio, G., 2001. Collar and root rot of olive trees caused by *Phytophthora megasperma* in sicily. Plant Dis. 85, 96.

Carlucci, A., Lops, F., Cibelli, F., Raimondo, M.L., 2015. *Phaeoacremonium* species associated with olive wilt and decline in Southern Italy. Eur. J. Plant Pathol. 141, 717–729.

Chatelet, D.S., Wistrom, C.M., Purcell, A.H., Rost, T.L., Matthews, M.A., 2011. Xylem structure of four grape varieties and 12 alternative hosts to the xylem-limited bacterium *Xylella fastidiosa*. Ann. Bot. 108, 73–85.

Corrado, G., Alagna, F., Rocco, M., Renzone, G., Varricchio, P., Coppola, V., Coppola, M., Garonna, A., Baldoni, L., Scaloni, A., Rao, R., 2012. Molecular interactions between the olive and the fruit fly Bactrocera oleae. BMC Plant Biol. 12, 1–17.

De Mendiburu, F., 2017. Agricolae: Statistical Procedures for Agricultural Research R Package Version 1. pp. 2–8. https://CRAN.R-project.org/package=agricolae.

Drenth, A., Wagels, G., Smith, B., Sendall, B., O'Dwyer, C., Irvine, G., Irwin, J.A.G., 2006. Development of a DNA-based method for detection and identification of *Phytophthora* species. Aust. Plant Pathol. 35, 147–159.

Edwards, K., Johnstone, C., Thompson, C., 1991. A simple and rapid method for the preparation of plant genomic DNA for PCR analysis. Nucleic Acids Res. 19, 1349.

Ferrante, A., Hunter, D.A., Reid, M.S., 2004. Towards a molecular strategy for improving harvesting of olives (*Olea europaea* L.). Postharvest Biol. Technol. 31, 111–117.
Frisullo, S., Camele, I., Agosteo, G.E., Boscia, D., Martelli, G.P., 2014. Brief historical account of olive leaf scorch (brusca) in the Salento peninsula of Italy and state-of-the-art of the olive quick decline syndrome. J. Plant. Pathol. 96, 441–449.
Fu, S., Arráez-Roman, D., Segura-Carretero, A., Menéndez, J.A., Menéndez-Gutiérrez, M.P., Micol, V., Fernández-Gutiérrez, A., 2010. Qualitative screening of phenolic compounds in olive leaf extracts by hyphenated liquid chromatography and preliminary evaluation of cytotoxic activity against human breast cancer cells. Anal. Bioanal. Chem. 397, 643–654.
Garrido, C., Carbú, M., Fernández-Acero, F.J., Boonham, N., Colyer, A., Cantoral, J.M., Budge, G., 2009. Development of protocols for detection of *Colletotrichum acutatum* and monitoring of strawberry anthracnose using qPCR. Plant Pathol. 58, 43–51.
Gayoso, C., Pomar, F., Novo-Uzal, E., Merino, F., Martínez de Ilárduya, O., 2010. The Ve-mediated resistance response of the tomato to *Verticillium dahliae* involves H_2O_2, peroxidase and lignins and drives PAL gene expression. BMC Plant Biol. 10, 232.
Gucci, R., Massai, R., Casano, S., Mazzoleni, S., 1999. Seasonal changes in the water relations of six Mediterranean woody species. Plant Biosyst. 133, 117–128.
Harper, S.J., Ward, L.I., Clover, G.R.G., 2010. Development of LAMP and QPCR methods for the rapid detection of *Xylella fastidiosa* for quarantine and field applications. Phytopathology 100, 1282–1288.
Herbette, S., Bouchet, B., Brunel, N., Bonnin, E., Cochard, H., Guillon, F., 2015. Immunolabelling of intervessel pits for polysaccharides and lignin helps in understanding their hydraulic properties in *Populus tremula* x *alba*. Ann. Bot. 115, 187–199.
Koudounas, K., Manioudaki, M.E., Kourti, A., Banilas, G., Hatzopoulos, P., 2015. Transcriptional profiling unravels potential metabolic activities of the olive leaf non glandular trichome. Front. Plant Sci. 6, 633.
Kraiselburd, I., Daurelio, L.D., Tondo, M.L., Merelo, P., Cortadi, A.A., 2013. The LOV protein of *Xanthomonas citri* subsp. citri plays a significant role in the counteraction of plant immune responses during citrus canker. PLoS One 8, e80930.
Lauvergeat, V., Lacomme, C., Lacombe, E., Lasserre, E., Roby, D., Grima-Pettenati, J., 2001. Two cinnamoyl-CoA reductase (CCR) genes from *Arabidopsis thaliana* are differentially expressed during development and in response to infection with pathogenic bacteria. Phytochemistry 57, 1187–1195.
Luvisi, A., Nicolì, F., De Bellis, L., 2017a. Sustainable management of plant quarantine pests: the case of olive quick decline syndrome. Sustainability 9, 659.
Luvisi, A., Aprile, A., Sabella, E., Vergine, M., Nicolì, F., Nutricati, E., Miceli, A., Negro, C., De Bellis, L., 2017b. *Xylella fastidiosa* subsp. pauca (CoDiRO strain) infection in four olive (*Olea europaea* L.) cultivars: profile of phenolic compounds in leaves and progression of leaf scorch symptoms. Phytopathol. Mediterr. 56, 259–273.
Maddox, C.E., Laur, L.M., Tian, L., 2010. Antibacterial activity of phenolic compounds against the pytopathogen *Xylella fastidiosa*. Curr. Microbiol. 60, 53–58.
Maroufi, A., Bockstaele, E.V., Loose, M.D., 2010. Validation of reference genes for gene expression analysis in chicory (*Cichorium intybus*) using quantitative real-time PCR. BMC Mol. Biol. 11, 15–27.
Martín, M.T., Cobos, R., Martín, L., López-Enríquez, L., 2012. qPCR Detection of *Phaeomoniella chlamydospora* and *Phaeoacremonium aleophilum*. Appl. Environ. Microbiol. 78, 3985–3991.
Martín, M.T., Cuesta, M.J., Martín, L., 2014. Development of SCAR primers for PCR assay to detect *Diplodia seriata*. Int. Sch. Res. Notices 2014, 824106.
Martelli, G.P., 2016. The current status of the quick decline syndrome of olive in Southern Italy. Phytoparasitica 44, 1–10.
Medina, M.B., 2011. Determination of the total phenolics in juices and superfruits by a novel chemical method. J. Funct. Foods 3, 79–87.
Miedes, E., Vanholme, R., Boerjan, W., Molina, A., 2014. The role of the secondary cell wall in plant resistance to pathogens. Front. Plant Sci. 5, 358.
Mitra, P.P., Loqué, D., 2014. Histochemical staining of *Arabidopsis thaliana* secondary cell wall elements. J. Visualized Exp. 13, 87.
Mizutani, M., Ohta, D., Sato, R., 1997. Isolation of a cDNA and a genomic clone encoding cinnamate 4-hydroxylase from *Arabidopsis* and its expression manner in planta. Plant Physiol. 3, 755–763.
Moreira-Vilar, F.C., Siqueira-Soares, R., Finger-Teixeira, A., De Oliveira, D.M., Ferro, A.P., Da Rocha, G.J., Ferrarese, M.L., Wanderley, D.S., Ferrarese-Filho, O., 2014. The acetyl bromide method is faster, simpler and presents best recovery of lignin in different herbaceous tissues than klason and thioglycolic acid methods. PLoS One 9, e110000.
Nicot, N., Hausman, J.F., Hoffmann, L., Evers, D., 2005. Housekeeping gene selection for real-time RT-PCR normalization in potato during biotic and abiotic stress. J. Exp. Bot. 56, 2907–2914.
Ortega-Garcìa, F., Peragòn, J., 2009. The response of phenylalanine ammonia-lyase, polyphenol oxidase and phenols to cold stress in the olive tree (*Olea europaea* L. cv. Picual). J. Sci. Food Agric. 89, 1565–1573.
Petridis, A., Therios, I., Samouris, G., Koundouras, S., Giannakoula, A., 2012. Effect of water deficit on leaf phenolic composition gas exchange, oxidative damage and antioxidant activity of four Greek olive (*Olea europaea* L) cultivars. Plant Physiol. Biochem. 60, 1–11.
Quirantes-Piné, R., Lozano-Sánchez, J., Herrero, M., Ibáñez, E., Segura-Carretero, A., Fernández-Gutiérrez, A., 2012. HPLC-ESI-QTOF-MS as a powerful analytical tool for characterising phenolic compounds in olive-leaf extracts. Phytochem. Anal. 24, 213–223.
Quiroga, M., Guerrero, C., Botella, M.A., Barceló, A., Amaya, I., Medina, M.I., Alonso, F.J., de Forchetti, S.M., Tigier, H., Valpuesta, V., 2000. A tomato peroxidase involved in the synthesis of lignin and suberin. Plant Physiol. 122, 1119–1127.
Rodrigues, J.L.M., Silva-Stenico, M.E., Gomes, J.E., Lopes, J.R.S., Tsai, S.M., 2003. Detection and diversity assessment of *Xylella fastidiosa* in Þeld-collected plant and insect samples by using 16S rRNA and gyrB sequences. Appl. Environ. Microbiol. 69, 4249–4255.
Romanazzi, G., Murolo, S., Pizzichini, L., Nardi, S., 2009. Esca in young and mature vineyards: and molecular diagnosis of the associated fungi. Eur. J. Plant Pathol. 125, 277–290.
Rossi, L., Borghib, M., Francinia, A., Linb, X., Xieb, D.Y., Sebastiania, L., 2016. Salt stress induces differential regulation of the phenylpropanoid pathway in *Olea europaea* cultivars Frantoio (salt-tolerant) and Leccino (salt-sensitive). J. Plant. Physiol. 204, 8–15.
Saponari, M., Boscia, D., Nigro, F., Martelli, G.P., 2013. Identification of DNA sequences related to *Xylella fastidiosa* in oleander, almond and olive trees exhibiting leaf scorch symptoms in Apulia (Southern Italy). J. Plant. Pathol. 95, 668.
Schoch, G.A., Nikov, G.N., Alworth, W.L., Werck-Reichhart, D., 2002. Chemical inactivation of the cinnamate 4-hydroxylase allows for the accumulation of salicylic acid in elicited cells. Plant. Physiol. 130, 1022–1031.
Sun, Q., Greve, L.C., Labavitch, J.M., 2011. Polysaccharide compositions of intervessel pit membranes contribute to pierce's disease resistance of grapevines. Plant Physiol. 155, 1976–1987.
Taamalli, A., Arráez-Román, D., Ibañez, E., Zarrouk, M., Segura-Carretero, A., Fernández-Gutiérrez, A., 2012. Optimization of microwave-assisted extraction for the characterization of olive leaf phenolic compounds by using HPLC-ESI-TOF-MS/IT-MS(2). J. Agr. Food Chem. 60, 791–798.
Taamalli, A., Abaza, L., Arráez Román, D., Segura Carretero, A., Fernández Gutiérrez, A., Zarrouk, M., Nabil, B.Y., 2013. Characterisation of phenolic compounds by HPLC-TOF/IT/MS in buds and open flowers of 'Chemlali' olive cultivar. Phytochem. Anal. 24, 504–512.
Talhaoui, N., Gómez-Caravaca, A.M., León, L., de la Rosa, R., Segura-Carretero, A., Fernández-Gutiérrez, A., 2014. Determination of phenolic compounds of 'Sikitita' olive leaves by HPLC-DAD-TOF-MS: Comparison with its parents 'Arbequina' and 'Picual' olive leaves. LWT-Food Sci. Technol. 58, 28–34.
Tumber, K.P., Alston, J.M., Fuller, K.B., 2014. Pierce's disease costs California $104 million per year. Calif. Agric. 68, 20–29.
Wallis, C.M., Chen, J., 2012. Grapevine phenolic compounds in xylem sap and tissues are significantly altered during infection by *Xylella fastidiosa*. Phytopathology 102, 816–826.
Wallis, C.M., Wallingford, A.K., Chen, J., 2013. Grapevine rootstock effects on scion sap phenolic levels, resistance to *Xylella fastidiosa* infection, and progression of Pierce's disease. Front. Plant Sci. 4, 502.
Xu, L., Zhu, L., Tu, L., Liu, L., Yuan, D., Jin, L., Long, L., Zhang, X., 2011. Lignin metabolism has a central role in the resistance of cotton to the wilt fungus *Verticillium dahliae* as revealed by RNA-Seq-dependent transcriptional analysis and histochemistry. J. Exp. Bot. 15, 5607–5621.